DNA Damage and Repair Following *In Vitro* Exposure to Two Different Forms of Titanium Dioxide Nanoparticles on Trout Erythrocyte

Durairaj Sekar,[1] Maria Letizia Falcioni,[2] Gianni Barucca,[3] Giancarlo Falcioni[2]

[1]School of Advanced Studies "Ageing and Nutrition," University of Camerino, Italy

[2]School of Pharmacy and Health Products, University of Camerino, Italy

[3]Dipartimento di Scienze e Ingegneria della Materia, dell'Ambiente ed Urbanistica, Università Politecnica delle Marche, Ancona, Italy

Received 11 May 2011; accepted 10 September 2011

ABSTRACT: TiO_2 has been widely used to promote organic compounds degradation on waste aqueous solution, however, data on TiO_2 nanotoxicity to aquatic life are still limited. In this *in vitro* study, we compare the toxicity of two different families of TiO_2 nanoparticles on erythrocytes from *Oncorhynchus mykiss* trout. The crystal structure of the two TiO_2 nanoparticles was analyzed by XRD and the results indicated that one sample is composed of TiO_2 in the anatase crystal phase, while the other sample contains a mixture of both the anatase and the rutile forms of TiO_2 in a 2:8 ratio. Further characterization of the two families of TiO_2 nanoparticles was determined by SEM high resolution images and BET technique. The toxicity results indicate that both TiO_2 nanoparticles increase the hemolysis rate in a dose dependent way (1.6, 3.2, 4.8 μg mL^{-1}) but they do not influence superoxide anion production due to NADH addition measured by chemiluminescence. Moreover, TiO_2 nanoparticles (4.8 μg mL^{-1}) induce DNA damage and the entity of the damage is independent from the type of TiO_2 nanoparticles used. Modified comet assay (Endo III and Fpg) shows that TiO_2 oxidizes not only purine but also pyrimidine bases. In our experimental conditions, the exposure to TiO_2 nanoparticles does not affect the DNA repair system functionality. The data obtained contribute to better characterize the aqueous environmental risks linked to TiO_2 nanoparticles exposure.
 Environ Toxicol 21: 000–000, 2011.

Keywords: TiO_2 nanoparticle; rutile; anatase; trout erythrocyte; hemolysis; DNA damage and repair

INTRODUCTION

Nanotechnology, defined as a technique aimed to design, characterize and produce materials on a nanometer scale, is continuously expanding at a fast rate. The nanotechnology global market accounted for about $10.5 billion in 2006 (http://www.bccresearch.com/nanotechnology). In the last few years, the nomenclature associated with nanoscience and nanotechnology has been widely debated. A commonly used definition of nanomaterial (NM) referred to materials size ranging between 1 and 100 nm; however this definition gave rise to many uncertainties and inconsistencies. NM are now identified by the scientific community as all materials with a dimension under 100 nm. Nanoparticles (NP) are currently defined as single particles with a diameter $<$100 nm, so they are a subset of nanomaterials (Borm et al. 2006; Klaine et al., 2011).

Nanomaterials are used in a wide range of industries, including food, clothing, electronics, cosmetics, medicine, and agriculture (Nel et al., 2006). Although nanotechnology offers a lot of benefits, the extensive use and development of NM has intensified research efforts regarding toxicity.

Correspondence to: G. Falcioni; e-mail: giancarlo.falcioni@unicam.it

Published online in Wiley Online Library (wileyonlinelibrary.com). DOI 10.1002/tox.20778

Although there is increasing consensus of opinion on the potential risk of engineered NPs for the environment (Borm et al. 2006; Reeves et al., 2008; Jiang et al., 2009; Klaine et al., 2011), there is a lack of information on their potential toxic effects on aquatic organisms (Federici et al., 2007; Canesi et al., 2010). There is growing concern on the possible adverse effects on aquatic organisms even if it still remains questionable whether the entities of actual discharges is sufficient to cause severe environmental problems (Canesi et al., 2010).

Many of the substance previously considered biologically inert may promote toxic effects when in a nanoparticulate state (Reeves et al., 2008). Recent toxicological studies on engineered NPs have confirmed that NPs can be potentially dangerous because of their unique physico-chemical properties (Jiang et al., 2009). Engineered or natural NPs often exhibit special physicochemical properties and reactivities due to their small size and homogeneous composition, structure or surface characteristics (Oberdorster et al., 2005; Powers et al., 2006).

Most of the current literature on NPs toxicity comes from mammalian studies on respiratory exposure, or from *in vitro* assays with mammalian cells (Handy and Shaw, 2007; Iavinco et al., 2011; Freyre-Fonseca et al., 2011).

Among the different NPs, nanometer-sized titanium dioxide (TiO_2) powders play an important role because they are widely used in industry for different applications. In particular, TiO_2 is employed as a white pigment, opacifier and photocatalyst (Habibi et al., 2007; Sen et al., 2009). TiO_2 accounts for 70% of the total production volume of pigments worldwide. It provides whiteness and opacity to paints, plastics, papers, inks, foods, etc. It is also used in cosmetics where it helps to protect the skin from ultraviolet light (EPA, 2009).

For a long time TiO_2 was considered innocuous in particle toxicology but recent studies on TiO_2 have reported multiple specific characteristics coupled with unknown risks to human health (Li et al., 2008) and the environment (Navarro et al., 2008).

The aim of this study was to compare the effects of two different families of TiO_2 nanoparticles on *O. mykiss* trout erythrocytes. The nanoparticles differ for their crystalline form (anatase and rutile based) and size and were chosen for their potentially different level of toxicity. Indeed, anatase is observed to be more biologically active than rutile in terms of cytotoxicity or oxidative DNA damage (Hirakawa et al., 2004; Sato and Taya, 2006). Moreover, Jang et al. (2007) have shown that for TiO_2 particles ranging between 15 and 30 nm, the bactericidal effects increases as the size of nanoparticles decreases and the mass fraction of anatase increases. Considering these results, small anatase-based particles should be much more toxic than large rutile-based particles.

Erythrocytes are routinely used as a model to study the toxicity of new chemicals (Tiano et al., 2003; Prasanthi et al., 2005) because numerous compounds persist in circulating blood before reaching target organs (Li et al., 2008). Moreover, fish erythrocytes possess nuclei, mitochondria, and other organelles typical of somatic cells and can be easily isolated.

The specific potential toxicity of TiO_2 NPs on trout erythrocytes was determined at different cellular levels. Our interest was mainly focused on the ability of these NPs to affect hemolysis and DNA status. Experiments were carried out in three fundamental steps. First, some physical characteristics of the nanoparticles under study were determined by various analytical techniques. Then the influence of different amounts of the two TiO_2 nanoparticle forms on hemolysis was evaluated. Finally, the specific effect of the two different TiO_2 NPs on trout erythrocytes DNA was assessed by the comet assay (Collins, 2004). This test permits to detect single- and double-strand DNA breaks, alkali-labile sites, incomplete excision repair sites, and DNA-DNA cross-linking at individual cell level (Wozniak and Blasiak, 2003). Moreover, the effect of the two TiO_2 crystalline forms on DNA repair ability of trout erythrocytes was investigated.

MATERIALS AND METHODS

Materials

All reagents were of pure and analytical grade. TiO_2 nanoparticles, lucigenin, NADH as well as the enzyme superoxide dismutase (SOD EC1.15.1.1.) were purchased from Sigma-Aldrich. Endo III and Fpg enzymes were obtained from Prof. A. Collins (Institute for Nutrition Research, University of Oslo, Norway). Dulbecco's Modified Eagle medium (MEM) was purchased from Lifetech (Life Technologies, Palsley, Scotland).

Characterization and Preparation of NPs

In the present work, two different families of commercial TiO_2 nanoparticles (anatase and rutile based) were tested. Samples A1 and A2 were provided by Sigma–Aldrich with a declared purity of >99.7 and $>97\%$, respectively, and their properties are listed in Table I.

TiO_2 particles were characterized by different techniques. GC-MS and HPLC-DAD-ESI-MS measurements were performed to investigate the presence of organic impurities. GC-MS analyses were carried out using an Agilent Technologies 5973 N mass spectrophotometer and an Agilent Technologies 6890 N gas-chromatograph. HPLC-DAD-ESI-MS spectra were obtained on a Hewlett Packard 1090 Series II HPLC associated with a 1100 MSD HEWLETT PACKARD mass spectrophotometer. No organic impurities were found in the two NP batches.

TABLE I. Samples description

Trade Name	Treatment	Crystal Phase	BET Surface Area S ($m^2\ g^{-1}$)	BET Particle Size D (nm)	SEM Particle Size (nm)	Abbreviation Used in this Article
Titanium (IV) oxide 99.7%	None	Anatase	132.73	12	10–20	A1
Titanium (IV) oxide $\geq$ 97%	1% *M*n as dopant	Anatase/Rutile 20/80 (w/w)	20.75	68	20–150	A2

Chemical–physical properties of tested NPs.

The structural characterization of the samples was performed by X-ray diffraction (XRD), high resolution scanning electron microscopy (HR-SEM) and surface area analyses. XRD analyses were carried out on a Bruker D8 Advance diffractometer in Bragg-Brentano geometry at 40 kV and 40 mA using Cu Kα radiation. Quantitative information was deduced using rutile-anatase standard samples. High resolution observations were carried out on a field emission Zeiss Supra 40 scanning electron microscope. Surface area analysis was conducted by nitrogen adsorption on a Beckman coulter SA 3400 apparatus at an adsorption temperature of -196°C. Before measurements, samples were treated under high vacuum at 130°C for 2 h according to the Brunauer, Emmet and Teller (BET) method (Brunauer et al., 1938).

Stock suspensions were prepared in water at a concentration of 80 μg mL^{-1} and to avoid aggregation they were sonicated for 10 min. Further dilutions were required to reach the final concentrations used (1.6, 3.2, and 4.8 μg mL^{-1}). To investigate the tendency of the particles to aggregate, Dynamic Light Scattering (DLS) and Z-potential measurements were performed on the particles suspensions using a Malvern Zetazizer Nano Instrument (model ZEN3600).

Samples

Red blood cells were obtained from *Oncorhynchus mykiss* trout (~24 months old, 180–300 g weight) coming from the fish farm ''Eredi Rossi Silvio'' Sefro, (MC) Italy. Fishes were kept in tanks containing water from Scarsito river, a tributary of Potenza river, and fed with commercial fish food obtained from Hedrix S.p.A (Mozzecane, VR, Italy). Blood was withdrawn by syringe from the caudal tail vein into an isotonic medium [0.1 M phosphate buffer, 0.1 M NaCl, 0.2% citrate, 1 mM ethylenediaminetetraacetic acid (EDTA), pH 7.8]. At least three trouts were collected in each experiment and the blood obtained from them was always pooled to minimize individual variability. After removing plasma and buffy coat by centrifugation at 1000 $\times$ g for 10 min, erythrocytes were washed three times and suspended in isotonic buffer (pH 7.8). On the contrary, when the experiments were carried out under stress conditions, the pH was 6.3 (Villarini et al., 1998).

Hemolysis

To evaluate the hemolysis rate, the erythrocytes were suspended in the above mentioned isotonic buffer pH 7.8 ([Hb] = 40 mg mL^{-1}) at room temperature. The degree of hemolysis was determined spectrophotometrically at a wavelength of 540 nm, as previously described (Falcioni et al., 1987), either in the absence or presence of different amounts of TiO_2 nanoparticles (1.6, 3.2, 4.8 μg mL^{-1}). In particular, the hemolysis rate was determined using the following expression $100 \times A/10 \times A^* \times 100\%$; where A is the hemoglobin concentration present in the supernatant of the red cell suspension after centrifugation, and $A^* \times 100\%$ is the hemoglobin concentration obtained after complete lysis with 10 vol. distilled water at zero time of incubation. The hemolytic process was also followed in suspensions incubated for 10 min with TiO_2 nanoparticles and subsequently washed with isotonic buffer (pH 7.8).

Chemiluminescence Assay

Chemiluminescence (CL) determinations were performed using lucigenin as luminogenic probe sensitive to the superoxide radical (Murphy and Sies, 1990). CL was measured in an Autolumat LB953 (Berthold, Wildbad, Germany) using a reaction mixture containing 150 μM lucigenin, 100 μM NADH, 50 mM isotonic Tris-HCl (pH 7.8) and 10 μL of an erythrocytes suspension ([Hb]= 0.3 mg mL^{-1}) in the presence or absence (control) of 4.8 μg mL^{-1} TiO_2 NPs. The reaction was followed for 60 min and the results expressed in counts/minutes (cpm). To confirm the nature of the observed chemiluminescence signal, superoxide dismutase (0.5 μM) was added to the reaction system.

Single-Cell Gel Electrophoresis (Comet Assay)

To evaluate the genotoxic effect of the two families of TiO_2 nanoparticles, the alkaline comet assay was performed on nucleated trout erythrocytes as previously described (Moretti et al., 1998). This test consists of embedding cells in agarose, cell membranes are then removed (lysis) and the DNA allowed to unwind. After electrophoresis, DNA damage can be visualized using Fluorescence Microscopy. The extent of DNA damage is determined by measuring the

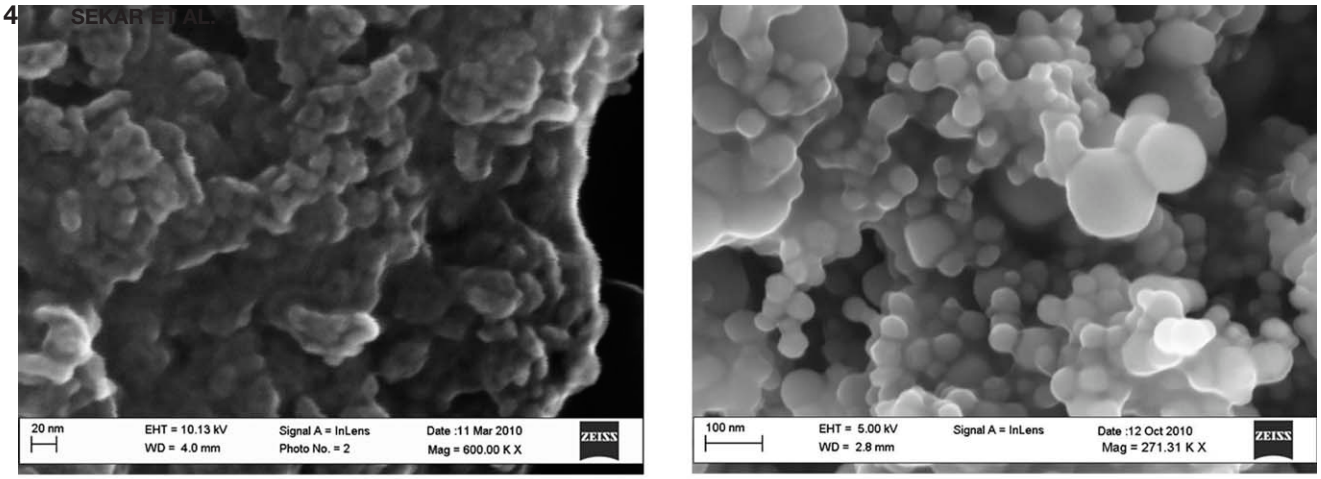

Fig. 1. SEM images of the TiO_2 nanoparticles. (a) A1 sample; (b) A2 sample.

displacement of genetic material between the cell nucleus (comet head) and the resulting tail. The alkaline version of comet assay reveals single- and double-strand breaks as well as alkali-labile sites (Wozniak and Blasiak, 2003).

Nearly 10^6 cells mL^{-1} were incubated for 1 h (RT) in isotonic buffer (see above) in the absence (control) or presence of TiO_2 NPs and the comet assay was then carried out. The TiO_2 NPs concentration used in the comet assays was the highest tested (4.8 μg mL^{-1}) in the hemolysis experiments. To better characterize the nature of DNA damage, the Endo III and Fpg modified version of the comet assay was performed (Falcioni et al., 2010). After lysis at pH 10, slides were immersed three times for 5 min in a washing solution containing 10 mM Tris–HCl, 100 mM NaCl, 1 mM EDTA, pH 7.4. Then, 100 μL of reaction buffer alone (RB) or plus 1 U of Endo III or Fpg was added to each slide. Subsequently, slides were incubated for 1 h at 37°C. RB contained: 40 mM HEPES, 0.1 M KCl, 0.5 mM EDTA, 0.2 mg mL^{-1} bovine serum albumin, pH 8. After keeping the slides at 4°C for 20 min to ensure the stability of the agarose film, electrophoresis and all the subsequent steps were performed as in the classic alkaline comet assay.

Positive controls were performed by preincubating erythrocytes at 4°C for 10 min with 10 mM H_2O_2 before suspending the cells in the low-melting agarose.

To assess the possible effect of TiO_2 nanoparticles on DNA repair systems, the erythrocyte suspensions (treated as described above) were kept for 1 h under oxidative stress conditions (isotonic buffer, pH 6.3 at 35°C), (Villarini et al., 1998). After incubation, cells were washed and resuspended in MEM. The DNA repair capacity was monitored over time. To verify the pertinence of the system, also untreated cells (control) were exposed to stress conditions and subsequently suspended in repair medium (MEM).

In all experiments, the DNA damage is expressed as percentage of DNA in the tail (% tail DNA) as suggested by Kumaravel and Jha (2006). % tail DNA was calculated as tail intensity/total comet intensity × 100.

Data (at least 150 scores per sample) are expressed as mean values ± standard error (SEM). Statistical analysis was carried out using one-way ANOVA followed by Student–Newman–Keuls test. A P-value <0.05 was considered statistically significant. Each experiment was performed three times. All the repetitions showed the same trend. One of them is reported as representative.

RESULTS

Characterization of TiO_2 Nanoparticles and Their Suspensions

The crystal structure of the TiO_2 nanoparticles was analyzed by XRD and the results are summarized in Table I. The A1 sample is composed of TiO_2 in the anatase crystal phase, while the A2 sample contains a mixture of both the anatase and the rutile form of TiO_2 in a 2:8 ratio.

SEM high resolution images of the two samples are shown in Figure 1. The A1 sample consists of nanoparticles almost spherical in shape and having a diameter ranging from 10 to 20 nm [Fig. 1(a)]. The A2 sample also consists of spherical particles but with a larger distribution of the particles size [Fig. 1(b)]. In particular, the particles diameter ranges from 20 to 150 nm, with a peak in the size distribution at about 60 nm.

The surface area of TiO_2 particles was determined by the BET technique and the theoretical particle size was calculated from the surface area using the following equation: $D = 6000/(\rho\, S)$.

This equation assumes spherical particles where D is the equivalent particle diameter in nanometers, ρ the particle density in g cm^{-3}, and S the specific surface area in m^2 g^{-1}. In Table I BET results are reported and it is evident that the equivalent particle diameter is consistent with the mean particle diameter deducible from SEM observations.

TABLE II. Dynamic light scattering and Zeta potential measurements

	Average Size (nm)	Polydispersity	Z-Potential (mV)
Immediately after sonication			
A1 stock suspen.(80 μg mL^{-1}) (pH 6.3)	463 ± 9	0.32 ± 0.03	−43 ± 3
A1 diluted suspen.(4.8 μg mL^{-1}) (pH 7.8)	650 ± 10	0.45 ± 0.08	−15 ± 1
A2 stock suspen.(80 μg mL^{-1}) (pH 6.3)	180 ± 10	0.19 ± 0.04	−65 ± 6
A2 diluted suspen.(4.8 μg mL^{-1}) (pH 7.8)	340 ± 40	0.21 ± 0.04	−12 ± 1
30 min after sonication			
A1 stock suspen. (80 μg mL^{-1}) (pH 6.3)	465 ± 9	0.31 ± 0.03	−43 ± 3
A1 diluted suspen.(4.8 μg mL^{-1}) (pH 7.8)	1200 ± 10	0.46 ± 0.08	−15 ± 1
A2 stock suspen.(80 μg mL^{-1}) (pH 6.3)	180 ± 10	0.20 ± 0.04	−65 ± 6
A2 diluted suspen.(4.8 μg mL^{-1}) (pH 7.8)	500 ± 10	0.24 ± 0.04	−12 ± 1

The average size of the agglomerates and the z-potential values for the stocks and diluted TiO_2 suspensions are shown. Measurements are performed immediately and 30 min after sonication

To evaluate the tendency of the TiO_2 particles to aggregate, DLS and Z-potential measurements were performed both on stocks and diluted suspensions (4.8 μg mL^{-1}). In particular, analyses were performed in two different moments: immediately and 30 min after sonication. The results, summarized in Table II, suggest a strong tendency of the anatase-based particles to aggregate. This tendency increases in the isotonic buffer (pH 7.8), where it is also seen that after 30 min the aggregates average size doubles. A similar behavior is observed for the rutile-based particles but the average size of the aggregates is smaller. It must be stressed that considering the polydispersity values (linked to the size dispersion width), the aggregates average sizes can be used only for comparative purposes and are not comparable with other techniques (Malvern Zetasizer Nano Series User Manual).

Hemolysis

The stability to lysis of trout erythrocytes is strongly dependent on temperature (Falcioni et al., 1987) and the hemolytic process can be followed, contrarily that for human erythrocytes, in a relatively short time even when cells are suspended in isotonic medium. For this reason, trout erythrocytes are excellent tools for studying the effects of new chemicals at the membrane level.

Figure 2 shows the time course of hemolysis in the presence and absence of different amounts of A1 NPs. The erythrocytes were suspended in isotonic buffer at pH 7.8 and incubated at RT. As can be observed, the presence of nanoparticles has a negative effect on the rate of hemolysis. It is necessary to point out that trout erythrocyte hemolysis occurs in the above conditions even in the absence of TiO_2 NPs. However, their presence accelerates this phenomenon in a dose-dependent manner. In particular, after 24 h of incubation, the extent of hemolysis was the following: control ~43%; 1.6 μg mL^{-1} A1 ~50%; 3.2 μg mL^{-1} A1 ~58%, and 4.8 μg mL^{-1} A1 ~61%. Treating cells with A2 TiO_2 NPs (1.6, 3.2, and 4.8 μg mL^{-1}), a similar effect was observed (data not shown). It is interesting to note that there was no met-Hb formation in the presence of both TiO_2 NPs after this 24-h incubation (data not shown). This information was derived from the hemolysates spectra recorded in the visible region (from 700 to 520 nm).

To test the possibility of removing NPs hemolytic effect, the cell suspensions were washed with the isotonic medium (pH 7.8) after 10 min of exposure to A1 or A2 TiO_2 nanoparticles (4.8 μg mL^{-1}). As shown in Figure 3, continuing the cells incubation at RT for 3 h, the effect of both TiO_2 nanoparticles on the hemolysis rate was removed upon washing the cells. No differences were observed in the hemolysis rates between the two crystalline forms of the TiO_2 NPs.

Superoxide Anion Production

Many cellular sources are involved in the production of reactive oxygen species (ROS) in general and superoxide

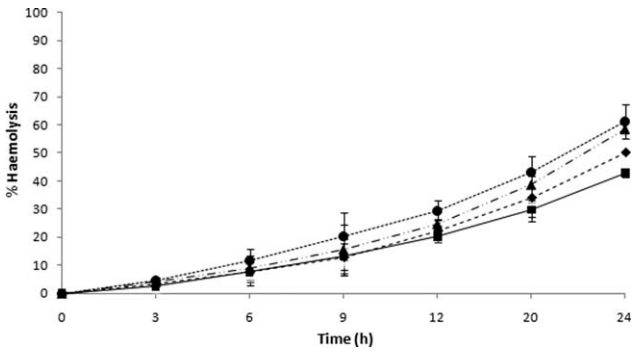

Fig. 2. Hemolysis vs. concentration. Time course of hemolysis of trout erythrocyte suspensions ([Hb]= 40 mg mL^{-1}) incubated in isotonic buffer pH 7.8 (RT) in the absence and presence of different amounts of A1 NPs. Data are expressed as mean values ± SD. The experiment was repeated three times. (■) Control; (◆) 1.6 μg mL^{-1} A1 sample; (▲) 3.2 μg mL^{-1} A1 sample; (●) 4.8 μg mL^{-1} A1 sample.

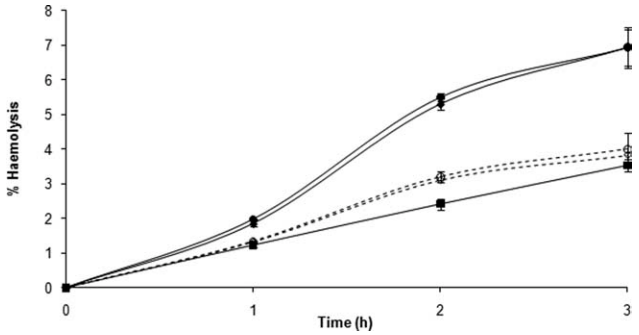

Fig. 3. Hemolysis. Time course of hemolysis of trout erythrocyte suspensions ([Hb] = 40 μg mL^{-1}) incubated in isotonic buffer pH 7.8 (RT) with 4.8 μg mL^{-1} of TiO_2 (A1 or A2). The erythrocyte suspension was washed or not after 10 min of TiO_2 exposure. Data are expressed as mean values ± SD. The experiment was repeated three times. (■) Control; (◆) A1 sample; (●) A2 sample; (◇) A1 sample washed cells; (○) A2 sample washed cells.

anion ($O_2^{-\cdot}$) in particular, including NAD(P)H-dependent electron transport chains, membrane-bound oxido-reductases, cytosolic xanthine oxidase, etc. The contribution of each source to $O_2^{-\cdot}$ production has been investigated in different tissues, but the exact involvement of these sources in ROS production remains unclear. However, studies suggest that a significant portion of ROS production is not derived from the mitochondria but is related to the presence of NAD(P)H (Bejma and Ji, 1999).

Lucigenin reaction with superoxide radical ($O_2^{-\cdot}$) produces a chemiluminescence (CL) signal. The level of CL can be used to measure the presence of superoxide in the medium under study (Murphy and Sies, 1990). It is important to emphasize that lucigenin is capable of passing through cell membranes and can be used to detect intracellular $O_2^{-\cdot}$ production (Li et al., 1999). Figure 4(a,b) are one representative set of tracings from a total of at least three experiments (having the same trend). The tracings show the kinetics of the lucigenin amplified chemiluminescence measured in a reaction system containing NADH and trout erythrocytes in the presence and absence of the nanoparticles under study. NADH addition was essential to record the CL signal, in other words the lucigenin-chemiluminescence signal was observed only when NADH was present in the suspension medium.

The data obtained using a fixed concentration of TiO_2 NPs (4.8 μg mL^{-1}) show that both crystalline forms do not significantly increase the area under the curve and thus superoxide production [Fig. 4(a,b)].

To confirm the origin of the observed CL, the experiments were repeated in the presence of superoxide dismutase ([SOD] = 0.5 μM). This enzyme catalyzes the dismutation of superoxide anion into oxygen and hydrogen peroxide. The CL signal was almost completely inhibited in the presence of SOD (data not shown).

DNA Damage and Repair

Experiments on DNA status were carried out using the comet assay. Data obtained from trout erythrocyte suspensions incubated in isotonic buffer (pH 7.8) at RT for 60 min in the presence of TiO_2 nanoparticles (4.8 μg mL^{-1}) are shown in Figure 5. A dose-dependent curve similar to hemolysis experiments was performed (data not shown), but the highest concentration was chosen to emphasize the potential different behavior between the two TiO_2 compounds. The % tail DNA was significantly increased when both TiO_2 nanoparticles (A1 and A2) were present. The

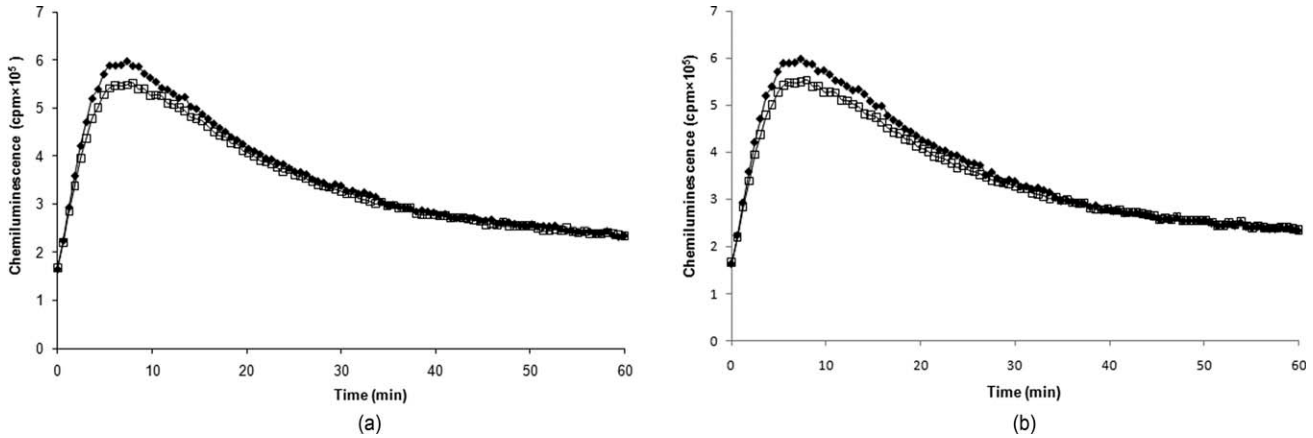

Fig. 4. Superoxide anion production. Kinetics of the lucigenin-amplified CL measured in the presence (◆) or absence (□) of 4.8 μg mL^{-1} A1 (a) or 4.8 μg mL^{-1} A2 (b). Reaction mixture contained 150 μM lucigenin, 100 μM NADH, 50 mM isotonic Tris-HCl (pH 7.8), and 10 μL erythrocyte suspension ([Hb] = 0.3 mg mL^{-1}). The reaction was followed for 60 min. Data are one representative set of tracings from a total of at least three experiments.

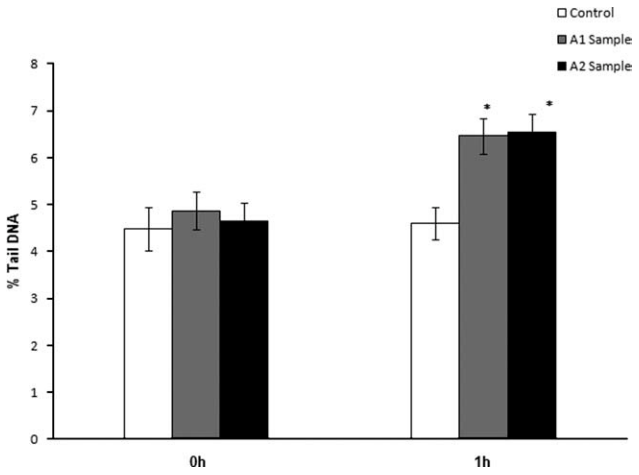

Fig. 5. DNA damage. % Tail DNA in erythrocytes after incubation with 4.8 μg mL^{-1} A1 or A2 nm in isotonic buffer, pH 7.8 (RT), for 1 h. Data are expressed as mean values ± SEM. At least 50 nuclei/slide were scored. The experiment was repeated at least three times. *$P < 0.05$ vs. control 1 h, A1 or A2 sample 0 h.

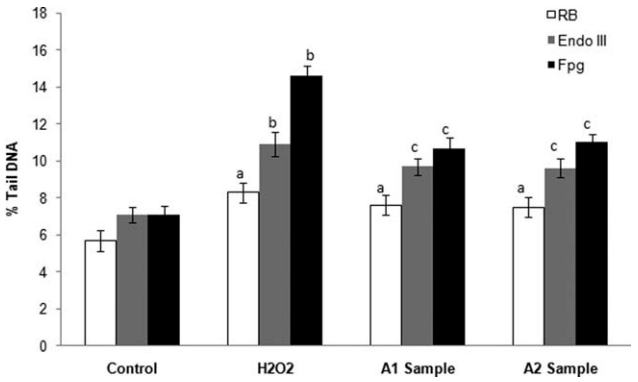

Fig. 6. Purine and pyrimidine oxidation. Effect of Endo III and Fpg on % Tail DNA damage in trout erythrocytes after incubation with 4.8 μg mL^{-1} A1 or A2 in isotonic buffer, pH 7.8 (RT), for 1 h. A 10-min exposure (4°C) to 10 mM H_2O_2 was used as positive control. Data are expressed as mean values ± SEM. At least 50 nuclei/slide were scored. The experiment was repeated at least three times. a. $P < 0.05$ vs. control RB. b. $P < 0.05$ vs. H_2O_2 RB. c. $P < 0.05$ vs. TiO_2 RB.

crystalline form did not influence the entity of DNA damage under our experimental conditions. DNA damage similar to the control was observed when washing cells after 10 min of TiO_2 exposure and continuing their incubation at RT for 60 min (data not shown).

To investigate the presence of DNA damage due to oxidation of pyrimidine and purine bases, Endo III and Fpg enzymes were used, respectively. These two enzymes recognize specific oxidative DNA damage: endonuclease III (Endo III) excises various pyrimidine derivates while formamido-pyrimidine DNA glycosilase (Fpg) excises oxidized purine residues (Collins, 2004). A statistically significant increase in the % tail DNA was observed in the presence of A1 and A2 TiO_2 NPs when the slides were incubated with both enzymes (Fig. 6). Figure 6 clearly indicates that the two TiO_2 crystalline forms oxidize in a similar way both pyrimidine and purine bases in trout erythrocyte DNA.

With or without enzymes, 10-min exposure to 10 mM H_2O_2 was found to increase DNA damage significantly (Fig. 6). This result confirms the pertinence/relevance of the system.

The effect of both nanoparticles was evaluated also during cell exposure to oxidative stress (Fig. 7). Stress was induced by incubating erythrocytes in isotonic buffer at pH 6.3 for 1 h at 35°C. Under these experimental conditions, oxidative stress is due both to the formation of superoxide radical and to the inactivation of glutathione peroxidase, as a consequence of Hb oxidation (see Falcioni et al., 1987). Trout erythrocytes incubated under stress conditions (1 h) undergo DNA damage (Villarini et al., 1998; Fedeli et al., 2004) which increases in a similar way in the presence of both TiO_2 NPs. To investigate the effect of the TiO_2 nanoparticles on the repair system, stressed cells were resuspended in an appropriate medium consisting of MEM and incubated at 10°C. After 1 h of incubation, but not after 30 min, DNA damage induced by stress conditions in the presence or absence of the two crystalline forms was repaired in a similar way (Fig. 7). Moreover, the significant reduction in DNA damage recorded after 1-h incubation under repair conditions versus the control under stress confirms the pertinence of the system (Fig. 7); in other words, stress

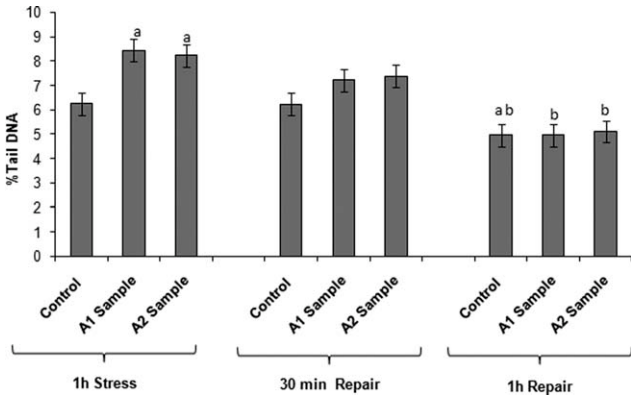

Fig. 7. DNA repair. Evaluation of DNA repair by the comet assay on trout erythrocytes incubated for 1 h under stress conditions (trout erythrocytes were suspended in isotonic buffer at pH 6.3 and incubated at 35°C) in the presence of 4.8 μg mL^{-1} TiO_2 (A1 and A2). The repair capacity was followed for 30- and 60-min incubating samples in MEM. Data are expressed as mean values ± SEM. At least 50 nuclei/slide were scored. The experiment was repeated at least three times. a. $P < 0.05$ vs. control 1 h stress. b. $P < 0.05$ vs. both TiO_2 1-h stress.

conditions induced a DNA damage in untreated cells (Control) that is repaired after 1 h of incubation in MEM.

DISCUSSION

Several works concerning the toxicity of TiO_2 NPs (Moore et al., 2006; Federici et al., 2007; Johnston et al., 2009; Gramowski et al., 2010), have shown that oxidative stress is a prominent feature of the response to TiO_2 NPs. Bhattacharya et al. (2009) reported that TiO_2 nanoparticles induce a concentration-dependent generation of intracellular reactive oxygen species (ROS) in BEAS-2B cells. In the same article, they also recorded a TiO_2 induced ROS formation in an acellular system (EPR studies). It has been observed that pretreatment with antioxidants diminishes the TiO_2 nanoparticle toxicity on a variety of cell types, including lung epithelial cells (Park et al., 2008), fibroblasts (Jin et al., 2008), and microglia (Long et al., 2006).

It is necessary to stress that the nanoparticle behavior is influenced by specific physical properties such as size, shape, surface area, crystal structure, etc. (Jiang et al., 2009; Fang et al., 2010). Studies showing increasing toxicity of nanoparticles compared to larger particles, have led to a widely assumed hypothesis that nanoparticles in general are more potent in causing damage (Donaldson et al., 2000).

Despite the knowledge that fish cells are recognized to be generally more prone to toxic and oxidative injury than similarly treated mammalian cells (Raisuddine and Jha, 2004; Rau et al., 2004), there is a scarcity of data concerning the potential detrimental effect of NPs on aquatic organisms. In particular, our interest focused on TiO_2 because it has been widely used even to promote the degradation of organic compounds in waste aqueous solution (Wold, 1993; Braydich-Stolle et al., 2009).

TiO_2 exists in two main crystalline forms called anatase and rutile showing different toxicity. Various studies point out that the anatase crystal form is more toxic than the rutile one (Wang et al., 2008; Braydich- Stolle et al.,2009; Wu et al., 2010). The ability of particles to exert toxicity at a variety of target sites is reliant on their transfer into blood. So far, little is known about the entry of nanoparticles and their transport through the blood stream to other organs. However, there is experimental evidence that particles may penetrate the red blood cell membrane by a still unknown mechanism (Rothen-Rutishauser et al., 2006).

An *in vivo* study clearly reported oxidative damage at gill, intestine and brain level in rainbow trout treated with TiO_2 nanoparticles (Federici et al., 2007). Gills are the major site for O_2 and CO_2 transfer in fishes, blood erythrocytes then transport these gases to and from the tissues.

In our study, two very different families of TiO_2 nanoparticles, different crystalline forms and mean sizes, were tested on trout erythrocytes. The results clearly show that both TiO_2 nanoparticles influence the hemolytic process of trout erythrocytes by increasing the hemolysis rate in a dose-dependent manner. Contrarily to what Aisaka et al. (2008) observed in human erythrocytes, anatase and rutile nano-scale TiO_2 induced hemolysis in a similar way under our experimental conditions (trout erythrocytes). Oxidative damage to red blood cell membranes may be a crucial event in the onset of hemolysis. Previously (Falcioni et al., 1987), we reported that the rate of oxidative hemolysis in trout erythrocytes is correlated with the rate of met-hemoglobin formation. However, preliminary data (not shown) seems to exclude an increase in lipid peroxidation due to the presence of TiO_2 NPs at erythrocyte plasma membrane level in our experimental condition. This is also in accordance with the redox status of hemoglobin that it is not influenced by the presence of both TiO_2 nanoparticles (unreported data). TiO_2 could destabilize the lipid raft, which may eventually lead to membrane deconstruction, and thus to hemolysis.

Furthermore, it is interesting to note that by washing the erythrocyte suspensions after 10 min of TiO_2 exposure, the nanoparticles effect on the hemolysis rate is reduced. This observation suggests that the nanoparticle uptake by trout erythrocytes is not as rapid as in human lung epithelial cells (Singh et al., 2007; Park et al., 2008).

Results from the comet assay indicate that both TiO_2 nanoparticles are genotoxic for trout erythrocytes. After 1-h incubation at RT both anatase (A1) and rutile-based (A2) TiO_2 NPs induce a statistically significant increase in DNA damage. The entity of DNA damage seems to be independent from the type of TiO_2 nanoparticle (Fig. 5). Some authors assumed that TiO_2 NPs promote ROS formation by TiO_2 catalytic chemical properties (hydroxyl radicals generation) (Hirano et al., 2005; Federici et al., 2007; Freyre-Fonseca et al., 2011; Thomas et al., 2011). The results obtained using the Endo III and Fpg modified version of comet assay seems to be consistent with this oxidative hypothesis. Both crystalline forms of TiO_2 nanoparticles are able to induce pyrimidine and purine bases oxidation (Fig. 6). Genotoxic effects of TiO_2 nanoparticles have been reported on goldfish skin by Reeves et al. (2008) and on a cell line derived from rainbow trout gonadal tissue by Vevers and Jha (2008). The induction of DNA strand breaks and moreover the increase in Fpg-sensitive sites broadly agree with the earlier observations made in the different cell types mentioned above, however, our study does not support what was observed on goldfish skin. Here, for the first time, we report a clear pyrimidine oxidation induced on trout erythrocytes DNA by both the TiO_2 NPs assessed.

Recent findings by Zucker et al. (2010) could contribute to justify the reported DNA damage. In particular, they observed that TiO_2 NPs uptaken by ARPE-19 cells tended to be compartmentalized and stored within the cell in ER and Golgi apparatus.

Accurate repair of DNA damage is of paramount importance for genome integrity. The genome is under constant threat of damage. To prevent loss or incorrect transmission

of genetic information, cells have developed numerous repair systems. The choice of the repair system to use depends on the cell-cycle phases and on the types of lesion. A number of DNA repair proteins (i.e. MED1, ATM, ATR, etc.) have been identified, some of them also impact the regulation of cell cycle and/or apoptosis. DNA double-strand breaks in S and G2 phase are repaired by homologous recombination using the intact sister chromatid. Damage affecting only one strand of DNA duplex may be repaired via excision repair pathways (Parsons 2003; Branzei and Foiani; 2008; Barlow at al., 2008).

In this study, the DNA repair system of trout erythrocytes exposed to both anatase (A1) and rutile-based (A2) TiO_2 NPs was assessed for the first time. As reported in Figure 7, 1-h exposure to TiO_2 nanoparticles under stress conditions does not affect erythrocyte DNA repair system functionality. After 1 h of incubation in MEM, DNA is completely repaired (Fig. 7).

In conclusion, our *in vitro* study compares the effects induced on trout erythrocytes by two different TiO_2 nanoparticles. Regardless of their potentially different levels of toxicity, they produce similar effects on trout red blood cells. TiO_2 nanoparticles increase the hemolysis rate. This increase does not seem to be correlated to direct oxidation of the lipids contained in the red blood cell membrane; TiO_2 nanoparticles do not induce an increased production of superoxide anion following addition of NADH. The exposure to TiO_2 nanoparticles induces DNA damage. This damage is related to oxidative stress since TiO_2 NPs promote the oxidation of pyrimidine and purine bases. Further studies should be carried out to better investigate the actual hemolysis mechanism and to further characterize the nature of DNA damage. The data obtained are important for the analysis of environmental risks produced by TiO_2 nanoparticles on fishes.

REFERENCES

Aisaka Y, Kawagichi R, Watanabe S, Ikeda M, Igisu H. 2008. Hemolysis caused by titanium dioxide particles. Inhal Toxicol 20:891–893.

Barlow JH, Lisby M, Rothstein R. 2008. Differential regulation of the cellular response to DNA double strand breaks in G1. Mol Cell 30:73–85.

Bejma J, Ji LL. 1999. Aging and acute exercise enhance free radical generation in rat skeletal muscle. J Appl Physiol 87:465–470.

Bhattacharya K, Davoren M, Boertz J, Schins RPF, Hoffmann E, Dopp E. 2009. Titanium dioxide nanoparticles induce oxidative stress and DNA-adduct formation but not DNA-breakage in human lung cells. Particle Fibre Toxicol 6:17–28.

Borm PJA, Robbins D, Haubold S, Kuhlbusch T, Fissan H, Donaldson K, Schins R, Stone V, Kreyling W, Lademann J, Krutmann J, Warheit D, Oberdorster E. 2006. The potential risks of nanomaterials: A review carried out for ECETOC. Particle Fibre Toxicol 3:11–46.

Branzei D, Foiani M. 2008. Regulation of DNA repair throughout the cell cycle nature reviews. Mol Cell Biol 9:297–308.

Braydich-Stolle LK, Schaeublin NM, Murdock RC, Jiang J, Biswas P, Schlager JJ, Hussain SM. 2009. Crystal structure mediates mode of cell death in TiO_2 nanotoxicity. J Nanopart Res 11:1361–1374.

Brunauer S, Emmett PH, Teller E. 1938. Adsorption of gases in multimoleculaar layers. J Am Chem Soc 60:309–319.

Canesi L, Ciacci C, Vallotto D, Gallo G, Marcomini A, Pojana G. 2010. In vitro effects of suspensions of selected nanoparticles (C60 fullerene, TiO_2, SiO_2) on Mytilus hemocytes. Aquat Toxicol 96:151–158.

Collins AR. 2004. The comet assay for DNA damage and repair. Mol Biotech 26:249–261.

Dodge JT, Mitchell C, Hanahan DJ. 1963. The preparation and chemical characteristics of hemoglobin-free ghosts of human erythrocytes. Arch Biochem Biophys 100:119–130.

Donaldson K, Stone V, Gilmour PS, Brown DM, MacNee W. 2000. Ultrafine particles: Mechanisms of lung injury. Philos Trans Royal 358:2741–2749.

EPA. 2009. External review draft, nanomaterial case studies: nanoscale titanium dioxide in water treatment and in topical sunscreen. United States Environmental Protection Agency. Available at:http://www.safenano.org/SingleNews.aspx?NewsId¼788 (accessed 09.10.10).

Falcioni G, Cincola G, Brunori M. 1987. Glutathione peroxidase and oxidative hemolysis in trout blood cells. FEBS Lett 221:355–358.

Falcioni ML, Nasuti C, Bergamini C, Fato R, Lenaz G, Gabbianelli R. 2010. The primary role of glutathione against nuclear DNA damage of striatum induced by permethrin in rats. Neurosci 16:168:2–10.

Fang X, Yu R, Li B, Somasundaran P, Chandran K. 2010. Stresses exerted by ZnO, CeO_2 and anatase TiO_2 nanoparticles on the *Nitrosomonas europaea*. J Coll Inter Sci 348:329–334.

Fedeli D, Berrettini M, Gabryelak T, Falcioni G. 2004. The effect of some tannins on trout erythrocytes exposed to oxidative stress. Mutat Res 10;563:89–96.

Federici G, Shaw BJ, Handy RD. 2007. Toxicity of titanium dioxide nanoparticles to rainbow trout (*Oncorhynchus mykiss*): Gill injury, oxidative stress, and other physiological effects. Aquatic Toxicol 84:415–430.

Folch J, Less M, Sloane-Stanley GH. 1957. A simple method for the isolation and purification of total lipids from animal tissues. J Biol Chem 226:497–509.

Freyre-Fonseca V, Delgado-Buenrostro NL, Gutiérrez-Cirlos EB, Calderón-Torres CM, Cabellos-Avelar T, Sánchez-Pérez Y, Pinzón E, Torres I, Molina-Jijón E, Zazueta C, Pedraza-Chaverri J, García-Cuéllar CM, Chirino YI. 2011. Titanium dioxide nanoparticles impair lung mitochondrial function. Toxicol Lett 25:202:111–119.

Gramowski A, Flossdorf J, Bhattacharya K, Jonas L, Lantow M, Rahman Q, Schiffmann D, Weiss DG, Dopp E. 2010. Nanoparticles induce changes of the electrical activity of neuronal networks on microelectrode array neurochips. Environ Health Perspect 118:1363–1369.

Habibi MH, Esfahani MN, Egerton TA. 2007. Photochemical characterization and photocatalytic properties of a nanostructure composite TiO_2 film. Inter J of Photoenergy: 13653–13661.

Handy RD, Shaw BJ. 2007. Toxic effects of nanoparticles and nanomaterials. Implication for public health, risk assesment and the public perception of nanotechnology. Health risk Soc 9:125–144.

Hirakawa K, Mori M, Yoshida M, Oikawa S, Kawanishi S. 2004. Photo-irradiated titanium dioxide catalyzes site specific DNA damage via generation of hydrogen peroxide. Free Radic Res 38:439–447.

Hirano K, Nitta H, Sawada K. 2005. Effect of sonication on the photocatalytic mineralization of some chlorinated organic compounds. Ultrason Sonochem 12:271–276.

Iavicoli I, Leso V, Fontana L, Bergamaschi A. 2011. Toxicological effects of titanium dioxide nanoparticles: A review of in vitro mammalian studies. Eur Rev Med Pharmacol Sci 15:481–508.

Jang H, Kim S. 2007. Effect of particle size and phase composition of titanium dioxide nanoparticles on the photocatalytic properties. J Nanoparticle Res 3:141–147.

Jiang J, Oberdorster G, Biswas P. 2009. Characterization of size, surface charge, and agglomeration state of nanoparticle dispersions for toxicological studies. J Nanopart Res 11:77–89.

Jin CY, Zhu BS, Wang XF, Lu QH. 2008. Cytotoxicity of titanium dioxide nanoparticles in mouse fibroblast cells. Chem Res Toxicol 21:871–1877.

Johnston HJ, Hutchison GR, Christensen FM, Peters S, Hankin S, Stone V. 2009. Identification of the mechanisms that drive the toxicity of TiO_2 particulates: The contribution of physicochemical characteristics. Part Fibre Toxicol 6:1–27.

Klaine SJ, Alvarez PJJ, Batley GE, Fernandes TF, Handy RD, Lyon DY, Mahendra S, McLaughlin MJ, Lead JR. 2008. Nanomaterials in the environment: Behavior, fate, bioavailability, and effects. Environ Toxicol Chem 27:1825–1851.

Konings AWT. 1984. Lipid peroxidation in liposomes. In: Gregoriadis G, editor. Liposomes Technology. Boca Raton: CRC Press. pp 139–161.

Kumaravel TS, Jha AN. 2006. Reliable comet assay measurements for detecting DNA damage induced by ionising radiation and chemicals. Mutat Res 605:7–16.

Li SQ, Zhu R, Zhu H, Xue M, Sun XY, Yao SD, Wang SL. 2008. Nanotoxicity of TiO_2 nanoparticles to erythrocyte in vitro. Food Chem Toxicol 46:3626–3631.

Li Y, Stansbury KH, Zhu H, Trush MA. 1999. Biochemical characterization of lucigenin (Bis-*N*-methylacridinium) as a chemiluminescent probe for detecting intramitochondrial superoxide anion radical production. Biochem Biophys Res Commun 262:80–87.

Long TC, Saleh N, Tilton RD, Lowry GV, Veronesi B. 2006. Titanium dioxide (P25) oxygen species in immortalized brain microglia (BV2): Implications for nanoparticle neurotoxicity. Environ Sci Technol 40:4346–4352.

Lowry OH, Rosebrough NJ, Faar AL, Randall RL. 1951. Protein measurement with the folin phenol reagent. J Biol Chem 193:265–275.

Moore MN. 2006. Do nanoparticles present ecotoxicological risks for the health of aquatic environment? Environ Intern 32:967–976.

Moore MN, Allen JI, McVeigh K. 2006. Environmental prognostics: An integrated model supporting lysosomal stress response as predictive biomarkers of animal health status. Mar Environ Res 61:278–304.

Moretti M, Villarini M, Scassellati-Sforzolini G, Santroni AM, Fedeli D, Falcioni G. 1998. Extent of DNA damage in density-separated trout erythrocytes assessed by the ''comet'' assay. Mutat Res 397:353–360.

Murphy ME, Sies H. 1990. Visible range low level chemiluminescence in the biological system. Method Enzymol 186:595–610.

Navarro E, Baun A, Behra R, Hartmann NB, Filser J, Miao AJ, Quigg A, Santschi PH, Sigg L. 2008. Environmental behavior and ecotoxicity of engineered nanoparticles to algae, plants, and fungi. Ecotoxicology 17:372–386.

Nel A, Xia T, Madler L, Li N. 2006. Toxic potential of materials at the nanolevel. Sci 311:622–627.

Oberdorster G, Maynard A, Donaldson K, Castranova V, Fitzpatrick J, Ausman K. 2005. Principles for characterizing the potential human health effects from exposure to nanomaterials: Elements of a screening strategy. Part Fibre Toxicol 6:2–8.

Park EJ, Yi J, Chung KH, Ryu DY, Choi J, Park K. 2008. Oxidative stress and apoptosis induced by titanium dioxide nanoparticles in cultured BEAS-2B cells. Toxicol Lett 180:222–229.

Parsons BL. 2003. MED1: A central molecule for maintenance of genome integrity and response to DNA damage. Proc Natl Acad Sci USA 100:14601–14602.

Powers KW, Brown SC, Krishna VB, Wasdo SC, Moudgil BM, Roberts SM. 2006. Research strategies for safety evaluation of nanomaterials. Part VI. Characterization of nanoscale particles for toxicological evaluation. Toxicol Sci 90:296–303.

Prasanthi K, Muralidhara Rajini PS. 2005. Morphological and biochemical perturbations in rat erythrocytes following in vitro exposure to Fenvalerate and its metabolite. Toxicol In Vitro 19:449–456.

Raisuddin S, Jha AN. 2004. Relative sensitivity of fish and mammalian cells to sodium arsenate and arsenite as determined by alkaline single cell gel electrophoresis and cytokinesis block micronucleus assay. Environ Mol Mutagen 44:83–89.

Rau MA, Whitaker J, Freedman JH, Giulio RT. 2004. Differential susceptibility of fish and rat liver cells to oxidative stress and cytotoxicity upon exposure to prooxidants. Comp Biochem Physiol C 137:335–342.

Reeves JF, Davies SJ, Dodd NJ, Jha AN. 2008. Hydroxyl radicals ($^{\cdot}OH$) are associated with titanum dioxide (TiO_2) nanoparticles-induced cytotoxicity and oxidative DNA damage in fish cells. Mutat Res 640:113–122.

Rothen-Rutishauser BM, Schurch S, Haenni B, Kapp N, Gehr P. 2006. Interaction of fine particles and nanoparticles with red blood cells visualized with advanced microscopic techniques. Environ Sci Technol 40:4353–4359.

Sato T, Taya M. 2006. Enhancement of phage inactivation using photocatalytic titanium dioxide particles with different crystalline structures. Biochem Eng J 28:303–308.

Sen G, ZhongBiao WU, WeiRong Z. 2009. TiO_2-based building materials: Above and beyond traditional applications. Chin Sci Bull 54:1137–1142.

Singh S, Shi T, Duffin R, Albrecht C, VanBerlo D, Hohr D, Fubini B, Martra G, Fenoglio I, Borm PJ, Schins RP. 2007.

Endocytosis, oxidative stress and IL-8 expression in human lung epithelial cells upon treatment with fine and ultrafine TiO_2: Role of specific area and of surface methylation of the particles. Toxicol Appl Pharmacol 222:141–151.

Thomas KV, Farkas J, Farmen E, Christian P, Langford K, Wu Q, Tollefsen KE. 2011. Effects of dispersed aggregates of carbon and titanium dioxide engineered nanoparticles on rainbow trout hepatocytes. J Toxicol Environ Health A 74:466–477.

Tiano L, Fedeli D, Santoni G, Davies I, Falcioni G. 2003. Effect of tributyltin on trout blood cells changes in mitochondrial morphology and functionality. Biochem Biophys Acta 1640:105–112.

Villarini M, Moretti M, Damiani E, Greci L, Santroni AM, Fedeli D, Falcioni G. 1998. Detection of DNA damage in stressed trout nucleated erythrocytes using the comet assay: Protection by nitroxide radicals. Free Radic Biol Med 24:1310–1315.

Wang J, Chen C, Liu Y, Jiao F, Li W, Lao F, Li Y, Li B, Ge C, Zhou G, Gao Y, Zhao Y, Chai Z. 2008. Potential neurological lesion after nasal instillation of TiO_2 nanoparticles in the anatase and rutile crystal phases. Toxicol Lett 183:72–80.

Wold A. 1993. Photocatalytic properties of TiO_2. Chem Mater 5:280–283.

Wozniak K, Blasiak J. 2003. In vitro genotoxicity of lead acetate: Induction of single and double DNA strand breaks and DNA–protein cross-links. Mutat Res 535:127–139.

Wu J, Sun J, Xue Y. 2010. Involvement of JNK and P53 activation in G2/M cell cycle arrest and apoptosis induced by titanium dioxide nanoparticles in neuron cells. Toxicol Lett 199:269–276.

Zucker RM, Massaro EJ, Sanders KM, Degn LL, Boyes WK. 2010. Detection of TiO_2 nanoparticles in cells by flow cytometry. Cytometry A 77A:677–685.